ChemComm

Accepted Manuscript

This article can be cited before page numbers have been issued, to do this please use: J. Mathew, Y. Nakajima, Y. Choe, Y. Urabe, W. Ando, K. Sato and S. Shimada, *Chem. Commun.*, 2016, DOI: 10.1039/C6CC01665K.

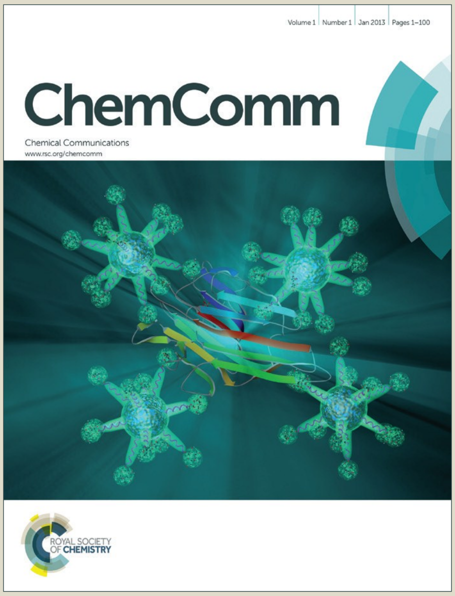

ROYAL SOCIETY OF CHEMISTRY

www.rsc.org/chemcomm

View Article Online
DOI: 10.1039/C6CC01665K

Journal Name

COMMUNICATION

Olefin Hydrosilylation Catalyzed by Cationic Nickel(II) Allyl Complexes: Non-Innocent Allyl Ligand-Assisted Mechanism

Received 00th January 20xx,
Accepted 00th January 20xx

DOI: 10.1039/x0xx00000x

www.rsc.org/

J. Mathew,[a] Y. Nakajima,*[b] Y.-K. Choe,[a] Y. Urabe,[b] W. Ando,[b] K. Sato[b] and S. Shimada[b]

The arene-supported cationic nickel allyl complexes serve as good catalysts for olefin hydrosilylation at room temperature. Detailed mechanistic studies based on experiments and DFT calculations support the novel mechanism, which includes the facile Si-H bond cleavage and Si-C bond formation, assisted by a non-innocent allyl ligand.

The hydrosilylation reaction is an efficient method for the formation of organosilicon compounds and represents one of the most important reactions in the silicon chemistry. Thus far, active studies have been continuously performed in this field using various transition metal catalysts such as precious metals (Pt, Rh, Ru etc.)[1,2] as well as earth-abundant non-precious metals (Fe[3], Co[4], Ni[5,6], etc.). Through these studies, several hydrosilylation mechanisms have been disclosed until now. One of the most important mechanism is the Chalk-Harrod/modified Chalk-Harrod mechanism, which normally operates in precious metal-catalyzed systems.[7] Although the utility of these systems are nowadays widely recognized both in the laboratory and in large-scale industrial applications, it is also reported that the system often accompanied by side reactions, leading to the decrease in the reaction selectivity. For early-transition metal and lanthanide catalyzed systems, σ-bond metathesis process is proposed.[8] Since this mechanism proceeds with fewer by-products, the development of this system significantly contributed to the design of highly selective hydrosilylation processes. Recently, a novel mechanism including a cationic ruthenium silylene complex as a key species was proposed by Tilley and Glaser.[9] The system successfully demonstrated the selective monoalkylation of primary silanes $RSiH_3$. As a result, the study has opened up the way to a new selective hydrosilylation reaction.

As seen from above mentioned studies, identification of a new mechanism for catalytic hydrosilylation can bring an important breakthrough to the conventional hydrosilylation chemistry, and thus is of great importance for the design of new catalysts, which enables to develop more efficient and selective systems. In this study, it was revealed that cationic nickel allyl complexes **1a-d** (Figure 1) successfully attain selective monoalkylation of secondary silanes, R_2SiH_2. Detailed mechanistic study using DFT methods suggested the novel Ni(II) catalyzed hydrosilylation mechanism including a unique function of a non-innocent allyl ligand, which account for the observed unique reaction selectivity.

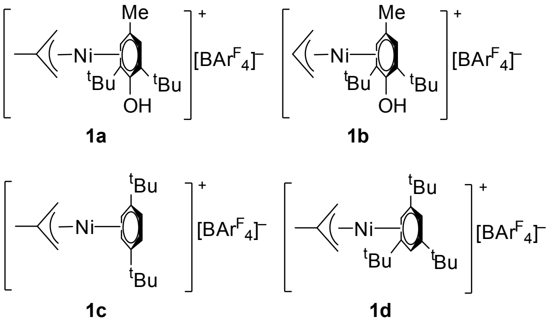

BAr^F_4 = $B(3,5\text{-}(CF_3)_2(C_6H_3))_4$

Figure 1. Complexes **1a**-**d**.

Complex **1b**, which has been established as a good diene polymerization catalyst, is easily prepared by the reaction of $[Ni(\eta^3\text{-}C_3H_5)Cl]_2$ with $NaBAr^F_4$ (BAr^F_4 = $B\{3,5\text{-}(CF_3)_2(C_6H_3)\}_4$).[10] Complexes **1a**, **1c**, and **1d** were similarly synthesized using a commercially available nickel precursor $[Ni(\eta^3\text{-}CH_2C(CH_3)CH_2)Cl]_2$ (Scheme 1).

In the presence of 0.5 mol% of the catalyst 1a, 1-octene was successfully hydrosilylated with various silanes at room temperature. The results of the reactions are summarized in

---

[a] Nanomaterials Research Institute, Research Centre for Computational Design of Functional Materials
National Institute of Advanced Industrial Science and Technology (AIST)
Tsukuba Central 2, 1-1-1 Umezono, Tsukuba, Ibaraki 305-8565, Japan
[b] Interdisciplinary Research Centre for Catalytic Chemistry
National Institute of Advanced Industrial Science and Technology (AIST)
Tsukuba Central 5, 1-1-1 Higashi, Tsukuba, Ibaraki 305-8565, Japan

Electronic Supplementary Information (ESI) available: [Experimental and theoretical details]. See DOI: 10.1039/x0xx00000x

View Article Online
DOI: 10.1039/C6CC01665K

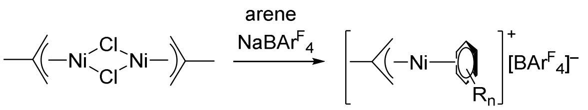

1a (56%), **1c** (18%)
1d (18%)

Scheme 1. Synthesis of **1a**, **1c**, and **1d.**

Table 1. Hydrosilylation of 1-octene with $RSiH_3$ (R = *n*Hex, *n*Oct) slowly proceeded to form the corresponding monohydrosilylated product $R(n\text{Oct})SiH_2$ and dihydrosilylated product $R_2(n\text{Oct})SiH$ in the total yield of ca 40% at room temperature after 24 h (entries 1,2). In these reactions, 1-octene also underwent isomerization to give a mixture of internal olefins and was completely consumed after the reaction, whereas unreacted $RSiH_3$ remained. In contrast, hydrosilylation of 1-octene with secondary silanes R_2SiH_2 quickly proceeded. For example, hydrosilylation of 1-octene with Et_2SiH_2 completed within 30 min under the same reaction conditions to selectively form monohydrosilylated product $Et_2(n\text{Oct})SiH$ in 75% yield as well as trace amounts of $Et_2(n\text{Oct})_2Si$ (1%) and $Et(n\text{Oct})_2SiH$ (2%) (entry 3). $Et(n\text{Oct})_2SiH$ is likely to be formed by the redistribution of the Et groups on the Si atom.[6] In this reaction, olefin isomerization was also detected. It should be noted that **1a** also catalysed hydrosilylation of 1-octene with Et_2SiH_2 even at lower catalyst loading of 0.1 mol% to selectively give $Et_2(n\text{Oct})SiH$ (68%) in 2.5 h (entry 4). Using $(n\text{Pen})_2SiH_2$ and $(n\text{Hex})_2SiH_2$, with bulkier substituents, hydrosilylation of 1-octene proceeded slowly but resulted in the formation of the corresponding monohydrosilylated products, $(n\text{Pen})_2(n\text{Oct})SiH$ and $(n\text{Hex})_2(n\text{Oct})SiH$ with high selectivities in high yields (90% and 96%, respectively; entries 5,6). Unfortunately, reactions using bulky tertiary silanes did not proceed. Furthermore, the hydrosilylation reactions were not successful to quantitatively recover 1-octene when using either Ph_2SiH_2 or $PhSiH_3$, which probably deactivates the catalyst by coordinating with the active Ni center via π-bonding of the Ph ring. Olefins with coordinating amino or sulphide groups (*N*,*N*-dimethylallylamine, but-3-en-1-yl(phenyl)sulfane) and coordinating solvents (acetonitrile, THF) could not be utilized, either. On the other hand, styrene was successfully hydrosilylated with Et_2SiH_2 to quantitatively give a mixture of α- and β-silylated products (entry 7).

To check the effect of the ligands on the catalytic activity, the hydrosilylation reaction of 1-octene with Et_2SiH_2 was performed using catalysts **1b**-**d**. Complex **1b**, which has an allyl group instead of a methallyl group, catalysed the hydrosilylation in a similar manner as **1a**; i.e. 1-octene was successfully hydrosilylated with Et_2SiH_2 in 30 min at 0.5 mol% catalyst loading, yielding $Et_2(n\text{Oct})SiH$ (76%), $Et_2(n\text{Oct})_2Si$ (1%), and $Et(n\text{Oct})_2SiH$ (2%) (entry 8). Complex **1c** supported by 1,4-di-*tert*-butylbenzene also exhibited a similar catalytic activity under the same reaction conditions, leading to the formation of $Et_2(n\text{Oct})SiH$ (76%), $Et_2(n\text{Oct})_2Si$ (4%), and $Et(n\text{Oct})_2SiH$ (1%) (entry 9)On the other hand, the reaction proceeded rather slowly albeit with higher selectivity to form $Et_2(n\text{Oct})SiH$ (92%) along with small amounts of byproducts when using **1d**.

Table 1. Hydrosilylation of 1-octene with various silanes catalysed by **1**[a]

entry	silane	catalyst (mol%)	time	Product yields[b] (isolated yield)
1	$(n\text{Hex})SiH_3$	**1a** (0.5)	24 h	$(n\text{Hex})(n\text{Oct})SiH_2$ 29% (25%) $(n\text{Hex})(n\text{Oct})_2SiH$ 11% (6%)
2	$(n\text{Oct})SiH_3$	**1a** (0.5)	24 h	$(n\text{Oct})_2SiH_2$ 19% (17%) $(n\text{Oct})_3SiH$ 18% (9%)
3	Et_2SiH_2	**1a** (0.5)	30 min	$Et_2(n\text{Oct})SiH$ 75% (71%) $Et_2(n\text{Oct})_2Si$ 1% $Et(n\text{Oct})_2SiH$ 2%
4	Et_2SiH_2	**1a** (0.1)	2.5 h	$Et_2(n\text{Oct})SiH$ 68% (58%) $Et_2(n\text{Oct})_2Si$ 2% $Et(n\text{Oct})_2SiH$ trace
5	$(n\text{Pen})_2SiH_2$	**1a** (0.5)	2 h	$(n\text{Pen})_2(n\text{Oct})SiH$ 90% (86%)
6	$(n\text{Hex})_2SiH_2$	**1a** (0.5)	2 h	$(n\text{Hex})_2(n\text{Oct})SiH$ 96% (95%)
7[c]	Et_2SiH_2	**1a** (0.5)	6 h	$1\text{-}(PhC_2H_4)Et_2SiH$ 68% (68%) $2\text{-}(PhC_2H_4)Et_2SiH$ 32% (14%)
8	Et_2SiH_2	**1b** (0.5)	30 min	$Et_2(n\text{Oct})SiH$ 76% (72%) $Et_2(n\text{Oct})_2Si$ 1% $Et(n\text{Oct})_2SiH$ 2%
9	Et_2SiH_2	**1c** (0.5)	30 min	$Et_2(n\text{Oct})SiH$ 76% (75%) $Et_2(n\text{Oct})_2Si$ 4% $Et(n\text{Oct})_2SiH$ 1%
10	Et_2SiH_2	**1d** (0.5)	9 h	$Et_2(n\text{Oct})SiH$ 92% (91%) $Et_2(n\text{Oct})_2Si$ 2% $Et(n\text{Oct})_2SiH$ trace

[a]]**1** (0.0042 mmol, or 0.00084 mmol for entry 4), silane (0.84 mmol), olefin (0.84 mmol) in CH_2Cl_2 (4 mL) at 25 °C. [b] GC yield (Isolated yield). [c] Styrene was used as an olefin substrate.

It is likely that the bulky 1,3,5-tri-*tert*-butylbenzene kinetically stabilizes **1d** and thus suppresses the formation of other Ni species, which could catalyse unwanted side-reactions.

One of the characteristic features of this system is that the catalysts exhibit extremely high activity when secondary silanes were utilized as substrates and achieve the selective monoalkylation of secondary silanes. It was also confirmed that the observed unique selectivity did not change when using an excess amount of 1-octene. Motivated by these results, hydrosilylation of 1-octene with Et_2SiH_2 in the presence of 5 mol% of **1a** was monitored by ^1H NMR spectroscopy to shed light on the reaction mechanism. Considering 18e count of **1a**, dissociation of the arene ligand and/or elimination of the methallyl ligand as an isobutene are expected for the Si–H bond cleavage step in the conventional Chalk-Harrod and σ-bond methathesis mechanisms. However, surprisingly, complex **1a** was continuously observed without any deterioration through the reaction; i.e. complex **1a** was fully recovered even after further addition of both Et_2SiH_2 (200 equiv) and 1-octene (200 equiv), and the expected hydrosilylated product $Et_2(\text{Oct})SiH$ was obtained as a major product. It was also confirmed that the presence of Hg did not bring any deleterious effect on the

View Article Online
DOI: 10.1039/C6CC01665K

hydrosilylation reaction catalysed by **1a**. Thus, a possibility of the formation of active heterogeneous species was excluded.

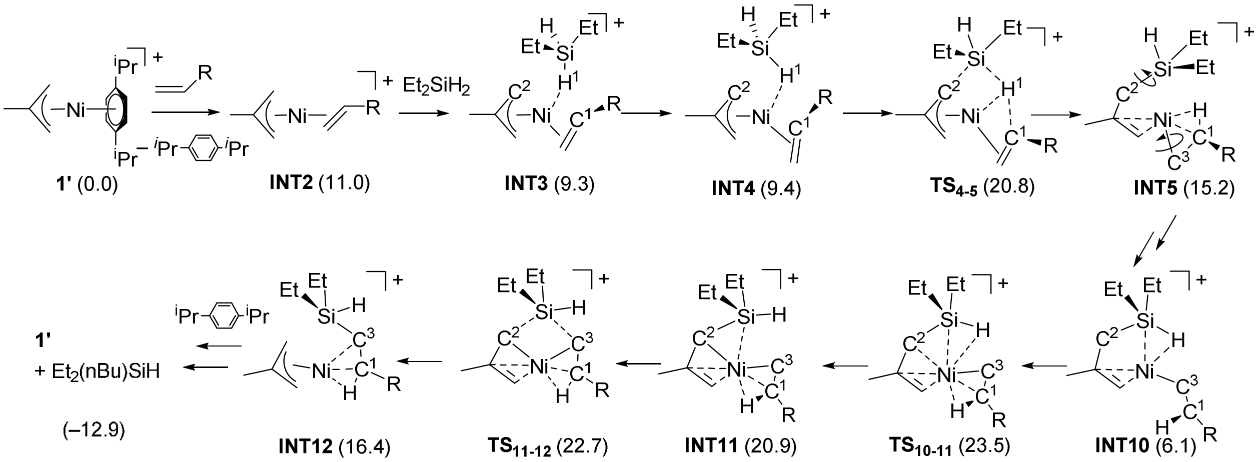

Figure 1. Summary of the structural changes of the reaction.

To investigate the mechanism, DFT calculations have been performed. In this calculation, a hydrosilylation reaction of 1-butene with Et$_2$SiH$_2$ was studied using a model catalyst [Ni(η^3-CH$_2$C(CH$_3$)CH$_2$)(η^6-1,4-iPr$_2$(C$_6$H$_4$)] (**1'**), which possesses 1,4-diisopropylbenzene as an arene ligand.

The reaction proceeds via ten transition states where the overall reaction energy is exothermic by –12.9 kcal/mol.[11] Figure 1 summarizes the important reaction steps of the mechanism, and all stationary points are depicted in Figure S4 in the supporting information. The reaction starts with the incorporation of 1-butene, which proceeds via dissociation of the arene ligand, to form π-allyl olefin complex **INT2**. In the next step, Et$_2$SiH$_2$ is incorporated via the Si–H bond to form σ-silane complex **INT3**. When going to **INT4**, the butene rotates for the better access of the silane H1 atom to the butene C1 atom. Then, the H1 atom approaches the C1 atom (C1–H1 = 1.37 Å), and the Si–H1 bond is lengthened to be 2.05 Å in **TS$_{4\text{-}5}$**, supporting the late transition state with a weak Si–H1 bonding interaction. Accompanied with this geometrical change, the methallyl C2 atom accesses the Si atom. As a result, the Si–C2 bond length becomes 2.56 Å, indicating the formation of a weak Si–C2 bonding interaction in **TS$_{4\text{-}5}$**. The single bond formation of the C1–H1 and Si–C2 bonds completed in **INT5**; i.e. the C1–H1 and Si–C2 bond lengths are 1.18 Å and 2.01 Å, respectively. The energy barrier of this step is 11.4 kcal/mol, and the free energy (ΔG) is 15.2 kcal/mol.

It is to be noted that the Ni–H and Ni–Si distances exhibit significantly longer values (1.5-1.7 Å and 2.4-2.8 Å, respectively) than the normal Ni–H (1.39-1.54 Å)[12,13] and Ni–Si (ca. 2.2 Å)[13,14] single bond lengths, through the Si–H bond cleavage process. The Mayer bond order analysis also supports the observed unique changes in the bonding nature along the reaction (Table 2). Upon going to **INT5** from **INT4**, the bond order of the Si–H1 bond decreases, whereas the bond orders of the C1–H1 and Si–C2 bonds increase. The rather small bond orders of the Ni–H1 and Ni–Si bonds (0.30 and 0.16, respectively) support no significant bonding interaction for those atom pairs in **INT5**. These results strongly indicate that the reaction proceeds via a novel mechanism other than either conventional Chalk-Harrod mechanism or σ-bond methathesis mechanism, where bond formations between the Ni center and the Si/H atom are expected (*vide infra*).

Table 2. Mayer bond order of **INT4**, **TS$_{4\text{-}5}$**, and **INT5**

	INT4	TS$_{4\text{-}5}$	INT5
Si–H1	0.50	0.01	–
C1-H1	0.01	0.45	0.63
Si–C2	–	0.24	0.61
Ni–Si	0.27	0.49	0.16
Ni-H1	0.46	0.42	0.30

INT5 further undergoes successive Si–C2 and Ni–C3 bond rotations to form **INT10**, in which the Ni atom possesses an agostic interaction with a Si–H bond. The process includes five transition states with relative energy barriers of 14 – 23 kcal/mol. Upon going to **INT11** from **INT10**, the Si–H agostic interaction dissociates from the Ni atom. As a result, this step is endothermic by 14.8 kcal/mol and proceeds via **TS$_{10\text{-}11}$** with the highest energy barrier (23.5 kcal/mol) through the whole reaction steps. The free energy of activation is reasonably comparable to the experimantal results, in which hydrosilylation reactions smoothly proceed at room temperature. In the structure of **INT11**, the Si–C2 bond is slightly elongated by 0.08 Å to be 2.04 Å and the Ni–C2 become shortened (2.15 Å). In the next step, the C3 atom of the butyl group approaches the Si atom. As a result, the Si–C3 distance becomes 2.89 Å, and the Si–C2 bond is simultaneously further elongated to be 2.21 Å in **TS$_{11\text{-}12}$**. The Si–C3 bond formation and Si–C2 bond cleavage occur upon going from **TS$_{11\text{-}12}$** to **INT12** in which the Si–C3 bond length is 2.04 Å. The energy barrier of this process is 22.7 kcal/mol. It is to be noted that the Ni and Si atoms again keep a certain distance (2.5 – 2.8 Å) through these reaction steps. After the dissociation of Et$_2$(nBu)SiH and recoordination of the arene ligand, **1'** is regenerated. We tentatively ascribe the observed unique mechanism to the cationic nature of the Ni center of **1'**; the NBO charge of the Ni in **1'** is 0.32, whereas the Pt atom in [Pt(SiH$_4$)(PPH$_3$)$_2$], which is calculated to undergo facile oxidative addition of a Si–H bond,[15] exhibits negative NBO

View Article Online
DOI: 10.1039/C6CC01665K

charge of –0.57. Since the cationic Ni atom preferably keeps a distance from the electropositive Si atom whose NBO charge is 1.31, the Si–H bond cleavage proceeds without any direct participation of the Ni(II) atom. Another notable feature of this process is the involvement of the allyl group as a non-innocent ligand. Orbital analysis suggested the involvement of C2 (2p) orbital for these steps. Figure 2a exhibits the 33th orbital of **INT4**, which includes σ-bonding interaction of Si (3s) and H1 (1s). This interaction is weakened, and the Si 3s orbital access the C2 2p orbital to form bonding interaction upon going to **INT5** from **INT4** (Figure 2b).

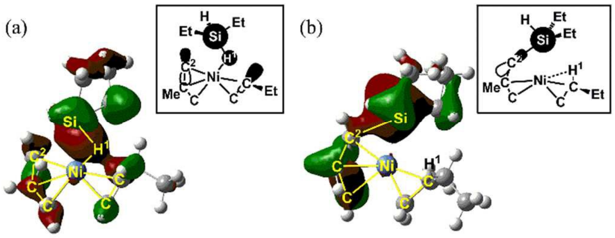

Figure 2. (a) 33th orbital of **INT4** (b) 34th orbital of **INT5**. Insets show schematic pictures of major orbital contributions.

The involvement of the C2 2p orbital is also supported on the Si–C3 bond forming step. Thus, as the Si atom access the C3 atom, the σ-bonding interaction between C2 (2p) and Si (3p) is concomitantly weakened upon going to **INT12** from **INT11** (Figure S8). It is likely that the cooperative bond forming and dissociating actions of the C2 atom compensate the energy change along the reaction. As a result, the Si–H cleavage and Si–C forming steps proceed with moderate energy barriers.

In the proposed mechanism, agostic Si–H and C–H bond interactions with the Ni atom play an important role. For examples, agostic interactions of Si–H and C–H bonds successfully stabilize the electron deficient Ni center in $\mathbf{TS_{10\text{-}11}}$. Furthermore, the agostic interactions facilitate the rotation of Si–C2 and Ni–C3 bonds. Therefore, it is reasonable that the system is not applicable to the hydrosilylation using tertially silanes, which cannot form stable intermediates through the Si–H agostic interaction after the Si–H bond cleavage. Indeed, optimization of **INT10** and $\mathbf{TS_{10\text{-}11}}$ using Et_3SiH was not successful due to their high instability. On the other hand, the effect of the agostic interactions does not explain the low reactivity of the catalytic system towards the hydrosilylation using primary silanes. To clarify this point, a DFT study on hydrosilylation of 1-butene with $EtSiH_3$ was performed. It was revealed that the rate-limiting step including the agostic Si–H bond dissociation proceeds via $\mathbf{TS}_{10\text{-}11}$* with a higher energy barrier compared with that in the Et_2SiH_2 system by 1 kcal/mol probably due to the strong agostic interaction between the less sterically hindered $EtSiH_2$ group and the Ni center. Indeed, the Ni–Si and Ni–H bond lengths in the transition state structure are 2.66 and 2.28 Å, respectively, which are 0.15 – 0.3 Å shorter than those in $\mathbf{TS_{10\text{-}11}}$. The energy difference might be one of the reasons for the low reactivity of monoalkylsilane in this system.

In summary, this study demonstrated the utility of cationic nickel allyl complexes as an olefin hydrosilylation catalyst. It is to be noted that the system exhibits high selectivity towards reactions using dialkylsilanes. The DFT study provides the evidence for the novel mechanism, which is assisted by the non-innocent allyl ligand for both the Si–H bond cleavage and the Si–C bond formation steps. Such a mechanism is different from either the conventional oxidative addition/reductive elimination or σ-bond metathesis process. The catalytic activity and the reaction selectivity are highly dependent on the type of the arene ligands in this system. Thus, the precise design of the reaction space using various arene ligands will be performed in due course for the further improvement of this system.

This work was supported by the "Development of Innovative Catalytic Processes for Organosilicon Functional Materials" project (PL: K.S.) from the New Energy and Industrial Technology Development Organization (NEDO).

Notes and references

1 B. Marciniec, H. Maciejewski, C. Pietraszuk, P. Pawluć in *Hydrosilylation: A Comprehensive Review on Recent Advances*, Springer, Berlin, 2009.

2 B. Marciniec, *Coord. Chem. Rev.*, 2005, **249**, 2374; A. K. Roy, *Adv. Organomet. Chem.*, 2008, **55**, 1; D. Troegel and J. Stohrer, *Coord. Chem. Rev.*, 2011, **255**, 1440; Y. Nakajima and S. Shimada, *RSC Adv.*, 2015, **5**, 20603.

3 J. Y. Wu, B. N. Stanzl and T. Ritter, *J. Am. Chem. Soc.*, 2010, **132**, 13214; A. M. Tondreau, C. C. H. Atienza, K. J. Weller, S. A. Nye, K. M. Lewis, J. G. P. Delis and P. J. Chirik, *Science*, 2012, **335**, 567.

4 M. Brookhart and B. E. Grant, *J. Am. Chem. Soc.*, 1993, **115**, 2151; C. Chen, M. B. Hecht, A. Kavara, W. W. Brennessel, B. Q. Mercado, D. J. Weix and P. L. Holland, *J. Am. Chem. Soc.*, 2015, **137**,13244.

5 Y. Kiso, M. Kumada, K. Tamao and M. Umeno, *J. Organomet. Chem.*, 1973, **50**, 297; Y. Chen, C. Sui-Seng, S. Boucher and D. Zargarian, *Organometallics*, 2005, **24**, 149; L. B. Junquera, M. C. Puerta and P. Valerga, *Organometallics*, 2012, **31**, 2175; I. Buslov, J. Becouse, S. Mazza, M. Montandon-Clerc and X. Hu, *Angew. Chem. Int. Ed.*, 2015, **54**, 14523.

6 V. Srinivas, Y. Nakajima, W. Ando, K. Sato and S. Shimada, *Catal. Sci. Technol.*, 2015, **5**, 2081; V. Srinivas, Y. Nakajima, W. Ando, K. Sato and S. Shimada, *J. Organomet. Chem.*, DOI 10.1016/j.jorganchem.2016.02.025.

7 A. J. Chalk and J. F. Harrod, *J. Am. Chem. Soc.*, 1965, **87**, 16.

8 P.-F. Fu, L. Brard, Y. Li and T. J. Marks, *J. Am. Chem. Soc.*, 1995, **117**, 7157; G. A. Molander and J. A. C. Romero, *Chem. Rev.*, 2002, **102**, 2161.

9 P. B. Glaser and T. D. Tilley, *J. Am. Chem. Soc.*, 2003, **125**, 13640.

10 J. Cámpora, M. del Mar Conejo, M. L. Reyes, K. Mereiter and E. Passaglia, *Chem. Commun.*, 2003, 78.

11 Figures S2 and S3 in the supporting information show the details.

12 W. Chen, S. Shimada, M. Tanaka, Y. Kobayashi and K. Saigo *J. Am. Chem. Soc.*, 2004, **126**, 8072; J. A. Hatnean, R. Beck, J. D. Borrelli and S. A. Johnson, *Organometallics*, 2010, **29**, 6077; P. Fischer, K. Götz, A. Eichhorn and U. Radius *Organometallics*, 2012, **31**, 1374.

13 T. Zell, T. Schaub, K. Radacki and U. Radius, *Dalton Trans.*, 2011, **40**, 1852.

14 S. N. MacMillan, W. H. Harman and J. C. Peters, *Chem. Sci.*, 2014, **5**, 590.

15 S. Sakaki, N. Mizoe, M. Sugimoto and Y. Musashi, *Coord. Chem. Rev.*, 1999, **190-192**, 933.

View Article Online
DOI: 10.1039/C6CC01665K

Graphical and textual abstract for the Table of Contents

Cationic nickel allyl complexes catalyse selective monohydrosilylation of α-olefins with *sec*-silanes via a unique mechanism assisted by a non-innocent allyl ligand.